

Title	Synthesis, characterization, and OLED application of oligo(p-phenylene ethynylene)s with polyhedral oligomeric silsesquioxanes (POSS) as pendant groups
Author(s)	Ervithayasuporn, Vuthichai; Abe, Junichi; Wang, Xin; Matsushima, Toshinori; Murata, Hideyuki; Kawakami, Yusuke
Citation	Tetrahedron, 66(48): 9348-9355
Issue Date	2010-10-10
Type	Journal Article
Text version	author
URL	http://hdl.handle.net/10119/9827
Rights	NOTICE: This is the author's version of a work accepted for publication by Elsevier. Vuthichai Ervithayasuporn, Junichi Abe, Xin Wang, Toshinori Matsushima, Hideyuki Murata, and Yusuke Kawakami, Tetrahedron, 66(48), 2010, 9348-9355, http://dx.doi.org/10.1016/j.tet.2010.10.009
Description	

Synthesis, characterization, and OLED application of oligo(*p*-phenylene ethynylene)s with polyhedral oligomeric silsesquioxanes (POSS) as pendant groups

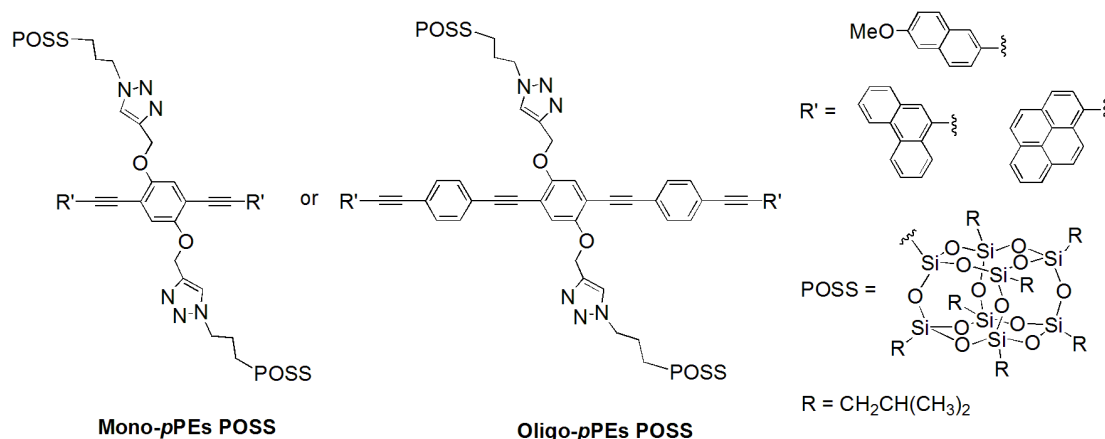
Vuthichai Ervithayasuporn,^{a,b,} Junichi Abe,^a Xin Wang,^a Toshinori Matsushima,^a Hideyuki Murata,^a and Yusuke Kawakami^a*

^aSchool of Materials Science, Japan Advanced Institute of Science and Technology (JAIST), 1-1 Asahidai, Nomi, Ishikawa 923-1292

^bDepartment of Chemistry, Faculty of Science, Mahidol University, Rama VI rd., Ratchathewi, Bangkok 10400, Thailand

* Corresponding author. Tel: +66-2-201-5126, Fax: +66-2-354-7151; e-mail address: scvuthichai@mahidol.ac.th (*V. Ervithayasuporn*).

Graphical abstract



Abstract

Two new classes of mono- and oligo(*p*-phenylene ethynylene)s grafted with polyhedral oligomeric silsesquioxanes (POSS) were synthesized *via* “click” chemistry and palladium-catalyzed Sonogashira cross-coupling. These materials with cubic silsesquioxanes are very robust with excellent thermal stability in air ($T_{5\% \text{ loss}} > 333^\circ\text{C}$) and exhibited $T_g > 80^\circ\text{C}$. All the compounds showed high photoluminescence with a range of blue emission and quantum yield up to 80% in the solution. Extended π conjugation molecules of oligo-*p*PEs POSS maintain relatively high PL quantum efficiencies in the solid state, compared to mono-*p*PEs POSS. A preliminary report is made of some of the materials as multilayer OLED components with active dopants PVK and PBD.

Keywords

p-phenylene ethynylene, Oligomer, Silsesquioxane, Photoluminescence, Light-emitting diode

1. Introduction

Polymeric and oligo(*p*-phenylene ethynylene)s (oligo-*p*PEs) with rigid rod-like structures^{1,2} are one class of conjugated π -electron molecules that have in many applications such as sensors,^{3,4} solar cells,^{5,6} biological uses,^{7,8} and electroluminescent materials.^{9,10} Oligo-*p*PEs also show a unique photoluminescence as monodisperse oligomers with precisely controlled repeating

units, when compared with polymeric system. Tuning the electronic properties of oligomers can be done usually by controlling the length of conjugation, directly substituted groups, and structural conformation.¹¹⁻¹⁵ Nevertheless, there are a few examples to functionalize terminal groups of oligomeric chain. Atienza *et al* first reported tuning electron transfer by a series of donor-bridge-acceptor systems through oligo-*p*PE molecular wires.¹⁶

Recently, polyhedral oligomeric silsesquioxanes (POSS) with rigid cage-like structures consisting of an inorganic Si-O-Si core and various organic substituents were found to be good candidates for many applications in materials science.¹⁷⁻²⁰ In organic light emitting diodes (OLEDs), when photo- and electroactive π -electron chromophores were incorporated into POSS framework, their photoluminescence quantum efficiencies and thermal properties were found to be significantly improved.^{21,24-26} The first introduction of silsesquioxane materials to OLEDs was achieved in 2003, when Xiao *et al* reported the higher brightness and external quantum efficiency of covalently anchored POSS at the chain-terminal of poly(phenylene vinylene).²¹ However, during the past five years, conventional reports of POSS in OLEDs have mainly explored the attachment of fluorescence molecules to the corners of hyperbranched POSS as a core. Octakis(dimethylsilyloxy)octasilsesquioxane is one candidate, easily reacted with any alkenyl-fluorophores through the hydrosilylation reaction to obtain full octa-functionalization. Our laboratory firstly proposed a perfect octacarbazole functionalized-POSS, which exhibited a strongly monomeric emission peak with the suppression of excimers even in the solid state.²² Cho *et al* reported an electroluminescent POSS-based nanoparticle. POSS cores were strongly confirmed to interrupt the aggregation of terfluorene hyperbranches in the matrix.²³ Froehlich *et al* proposed the same colour of emitters or a combination of different colours hydrosilylated to POSS.²⁴ However, these functionalities may show some intramolecular quenching and energy transfer due to the high flexibility of organic chain. Meanwhile, octa(vinyl)octasilsesquioxane is one promising molecule readily cross-coupling through Heck reaction with various haloaromatics. Extending conjugation on its rigid and reactive vinyl groups resulted in a change of electronic, morphologies, and amorphous properties, differed to small fluorophore analogues. Sellinger *et al* reported an 18% improvement in external quantum efficiencies, when connected with a

bromoaromatic hole transport material.²⁵ By introducing pyrene groups, Lo *et al* obtained the highest external quantum and current efficiencies of 2.63% and 8.28 cd/A, respectively.²⁶ Another rigidly functionalized-POSS goes to octa(phenyl)octasilsesquioxane derivatives containing highly functional groups on phenyl rings such as amino, bromo, and iodo functions.²⁷ For example, octa(bromophenyl)octasilsesquioxane was independently synthesized and reacted with the Grignard reagent in order to conjugate with oligophenylenes.^{28,29} However, their functionalization has encountered some difficulties such as uncontrolled reaction numbers, separation, and imprecise structures. A few reports of designing POSS as a pendant into conjugated molecules have been made. Miyake and Chujo recently reported that POSS wrapping along π -conjugated polymers could significantly enhance luminescence stabilities due to the steric effect of the POSS units.³⁰⁻³²

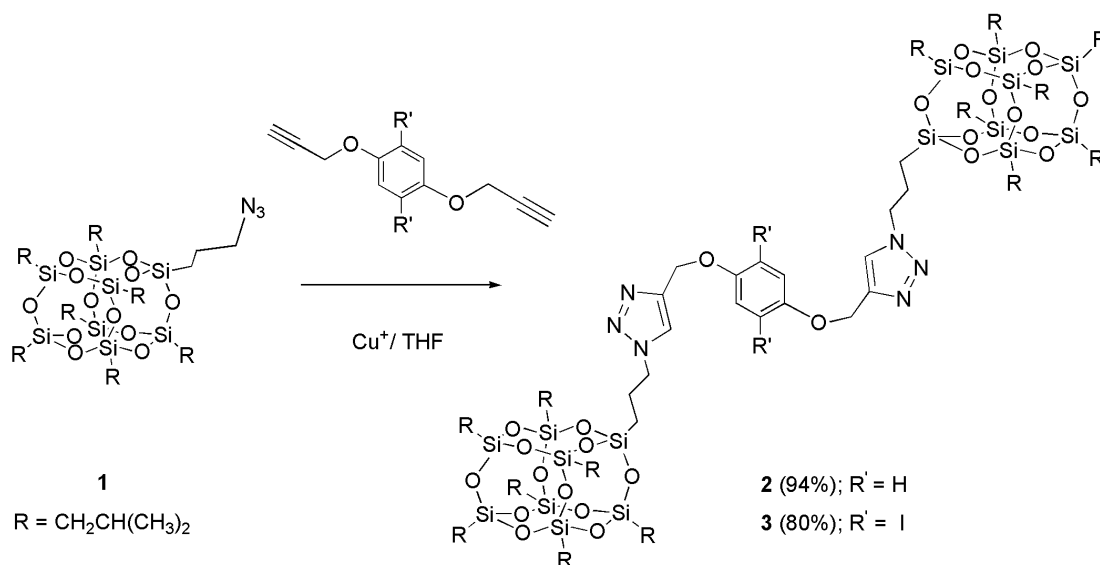
Herein, we report the synthesis of new series of mono- and oligo-*p*PEs POSS. Firstly, the novel 2-arm POSS (**3**) monomer was prepared *via* “click” chemistry and subsequent end-capping with various polycyclic aromatics by Sonogashira cross-coupling reaction to obtain *p*PE oligomers from deep blue to sky blue emission. In consequence, all desirable products were purified and given in an excellent yield with high thermal stability. These compounds were also found to be promising candidates in OLEDs as dopant materials.

2. Results and discussion

2.1 Synthesis

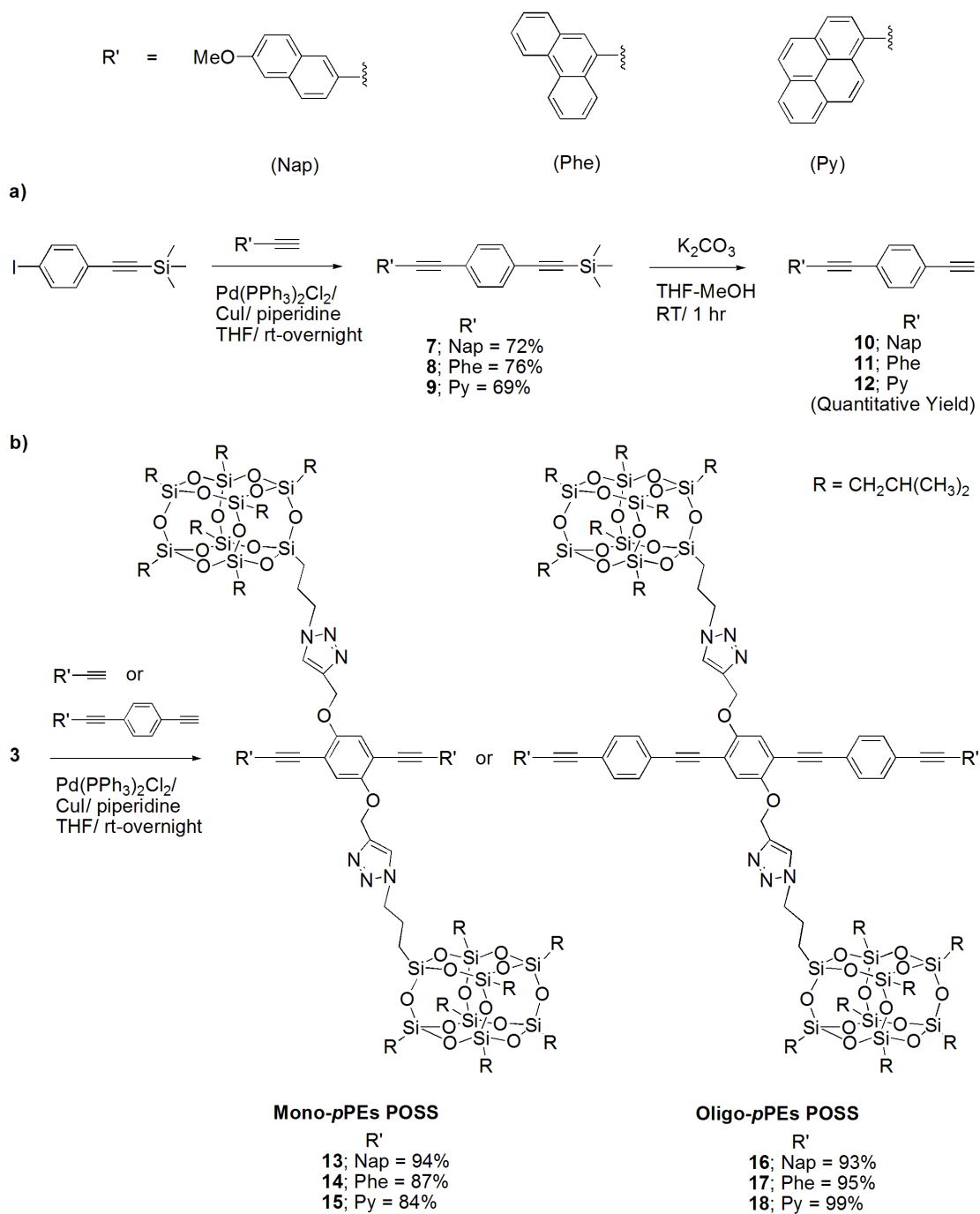
In order to evaluate the reaction condition, novel 2-arm POSS monomer (**2**) (Scheme 1) was preliminarily synthesized *via* “click” chemistry between freshly prepared mono azido-functionalized POSS (**1**)³³ and bis(propargyl)benzene. The 1,3-dipolar cycloaddition reaction was carried out in the presence of Cu⁺ (reduced form of CuSO₄ in sodium ascorbate) as an active catalyst. Compound **1** was completely consumed in 48 hours at 40°C to form the 1,4-regioisomer of 2-arm POSS product **2** (94 % yield). However, the similarly carried out reaction between **1** and 1,4-diiodo-2,5-bis(prop-2-ynyloxy)benzene was incomplete under the same reaction condition, evidenced by the presence of remaining starting materials. This failure can be explained by the steric effect on iodo-substituent benzene retarding an approach of “click” reaction. We further optimized the reaction conditions by

increasing the amount of catalyst, reaction time, and temperature. The complete reaction was finally observed in 5 days under reflux. Column chromatography successfully separated a pure form of 2-arm POSS monomer (**3**) in 80% yield.



Scheme 1 Cu^+ catalyzed double-click cycloaddition reactions: **2**,
 CuSO_4 -sodium ascorbate/ 40°C -2 days, 94% yield; **3**, CuSO_4 -sodium ascorbate/ Cu^0 /
 reflux-5 days, 80% yield.

To extend a *p*-phenylene ethynylene backbone for synthesizing oligo-*p*PEs POSS (**16**, **17**, and **18**), co-monomers (**10**, **11**, and **12**) have been prepared by using a “protected-alkyne route” (Scheme 2a). Firstly, ((4-iodophenyl)ethynyl)-trimethylsilane was cross-coupled with commercially available ethynyl polycyclic aromatic derivatives: 2-ethynyl-6-methoxy-naphthalene (**4**), 9-ethynyl-phenanthrene (**5**), and 1-ethynylpyrene (**6**) by Sonogashira cross-coupling reaction, where led to the formation of protected precursors (**7**, **8**, and **9**, respectively) in moderate yields. Subsequent treatment by methanolysis reaction with potassium carbonate cleaved the trimethylsilyl (TMS) group from the TMS-linked alkyne to give a quantitative yield of monomers (**10**, **11**, and **12**). These materials were available to use without further purification for constructing the higher order-structure of oligo-*p*PEs POSS.



Scheme 2 Pd(0)-catalyzed Sonogashira cross-coupling reaction leading to: a) polycyclic aromatic (*p*-phenylene ethynylene) monomers and b) mono- and oligo-*p*PEs POSS

For our approach to the synthesis of conjugated *para*-phenylene ethynylene based on POSS, two families of ethynyl polycyclic aromatics were readily used to grow oligomeric chain (Scheme 2b). The introduction of palladium-catalyzed

cross-coupling reaction between a 2-arm POSS (**3**) and monomers (**4**, **5**, and **6**) provided the new class of mono-*p*PEs POSS (**13**, **14**, and **15**) in excellent yield, respectively. Similarly, the reaction of **3** and freshly prepared materials (**10**, **11**, and **12**) gave a longer extended *p*PE backbone of oligo-*p*PEs POSS (**16**, **17**, and **18**), respectively.

2.2 Thermal properties

Table 1 Thermal properties of parent molecules, mono- and oligo-*p*PEs POSS

Compounds	$T_{5\%loss}$ (°C) ^a	T_g (°C)
7	255	
8	282	
9	311	
13	332	80
14	348	182
15	358	107
16	369	135
17	363	197
18	366	173

^aTGA was performed at a heating rate of 10°C/min under air atmosphere

The thermal stability of materials may be one criteria of the lifetime and durability of electronic devices. High temperature and oxygenated conditions usually decompose organic materials, possibly leading to a shorter lifetime of any device. Figure 1 shows that once mono- and oligo-*p*PEs possess the POSS as pendant groups, their $T_{5\%loss}$ were all above 330°C in air atmosphere. As well as, an improving the $T_{5\%loss}$ of all materials was by 47°C to 114°C, when compared to purely organic parent molecules. This actually proves that an inorganic silsesquioxane core could efficiently enhance the thermal stability and prolong the lifetime of materials. The glass transition temperature (T_g) is another important factor in determining the stability of OLED devices and their shelf lifetimes. The T_g values for these emitter functionalized POSS materials are all above 80°C as indicated in Table 1.

2.3 Photophysical properties

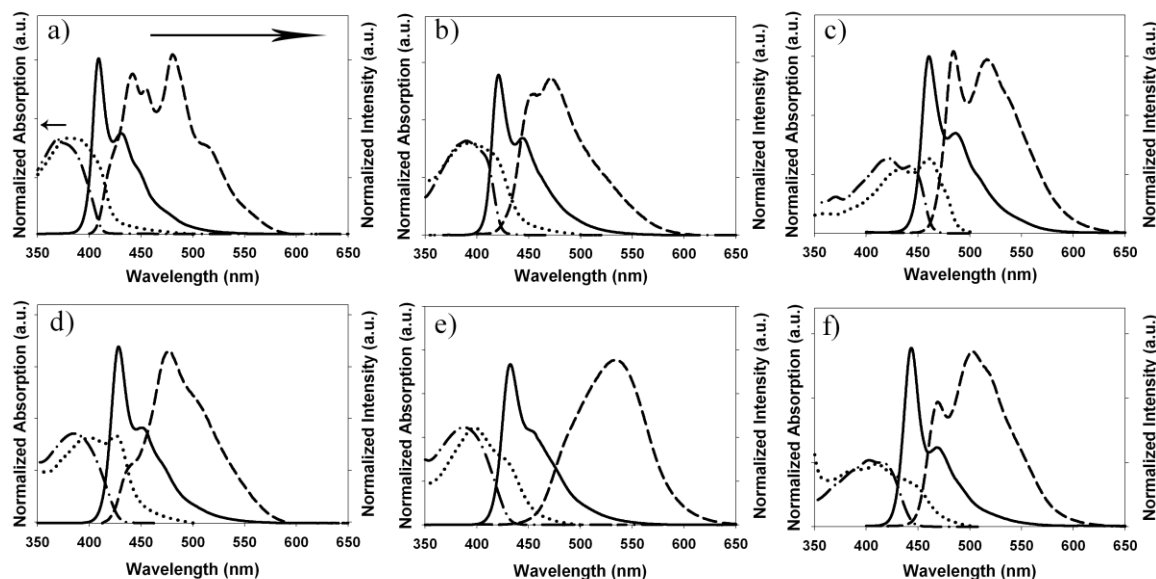


Figure 1 Absorption spectra in THF solution (dot) and dropped cast film (dash dot) and emission spectra in THF solution (solid) and dropped cast film (dash) of materials: a) **13**, b) **14**, c) **15**, d) **16**, e) **17**, and f) **18**.

Table 2 Maximum Absorption, Emission, and Photoluminescence quantum yield of mono- and oligo-*p*PEs POSS

Compounds	Solution ^a			Solid state		
	A_{\max} (nm)	Em_{\max} (nm) ^b	Φ	A_{\max} (nm)	Em_{\max} (nm) ^b	Φ
13	373	409	0.81	388	480	0.09
14	390	421	0.81	389	470	0.17
15	420	461	0.87	461	484	0.11
16	385	428	0.82	426	476	0.28
17	388	432	0.86	399	533	0.31
18	403	443	0.84	410	503	0.37

^aSolvent = THF (1×10^{-7} M); ^bExcitation wavelength = 350 nm; Φ , measurement done in excitation wavelength = 350 nm

Phenylene-ethynylene oligomers are typically fluorescent ($\Phi \approx 0.6-0.8$) and absorb strongly in the UV region.³⁴⁻³⁵ The absorption and emission bands shift to longer wavelengths upon extension of the conjugation. However, longer oligomers possess poor solubility and cause problems in the purification process. Alternatively, it is possible to extend the absorption spectral properties of these oligomers into the visible region *via* π conjugation with aryl groups.³⁶ In this study, the *p*-phenylene-ethynylene oligomer was terminally capped with numbers of polycyclic aromatics to extend and tune its photoresponsive nature. The solubilities of the desired products in organic solvents were also increased due to the presence of the grafted POSS units.

The solution-state absorption and fluorescence spectra of mono- and oligo-*p*PEs POSS were recorded in THF and are shown in Figure 1 and Table 2. By design, the band gap tuned from deep blue to sky blue was achieved in both mono- and oligo-*p*PEs POSS, where a red-shift of absorption and emission spectra was observed after the aromatic number of end-capping molecules was increased. In addition, the peak absorption and emission wavelengths of oligo-*p*PEs POSS (**16** and **17**) were red-shifted compared to the corresponding maxima for mono-*p*PEs POSS (**13** and **14**), respectively because of the extended conjugation in a main chain *p*PE. Interestingly, pyrene-linked molecules of **18** showed a blue-shift in both the absorption and emission spectra compared to mono-*p*PEs POSS (**15**).

The solid-state absorption and photoluminescence (PL) results are also plotted in Figure 1 and the data summarized in Table 2. The absorption and PL spectra of drop-cast films of **13-18** are red-shifted, compared to the solution state. These spectroscopic features display arising from interchain orbital interactions, generally referred to as aggregation bands. Similarly, the quantum efficiency of these aggregated systems is dramatically reduced in the solid-state. However, the extended π conjugation molecules of oligo-*p*PEs POSS (**16**, **17**, and **18**) maintain relatively high PL quantum efficiencies when compared to mono-*p*PEs POSS (**13**, **14**, and **15**). We suggest that without the elongated π backbone of *p*PE, the polyaromatic at the chain-terminal mono-*p*PEs POSS possesses a stronger π - π interaction with neighbor molecules, which led to self-quenching.

2.4 Optical devices

EL devices named as dye-doped OLEDs were fabricated for the emission characteristics of dopant **15** and **18**. However, two types of OLED structures were made to optimize device efficiency, designed as devices A and B. While the OLED structure of device A for **15** was composed of ITO/PEDOT:PSS/dopant(1-8% w/w):PBD:PVK/MPT/LiF/Al, device B of **18** was ITO/PEDOT:PSS/PVK/dopant(3-12% w/w):PBD:PVK/MPT/LiF/Al. The normalized EL spectra driven at current density of 0.1 mA/cm^2 with varied dopant concentrations are shown in Figure 2.

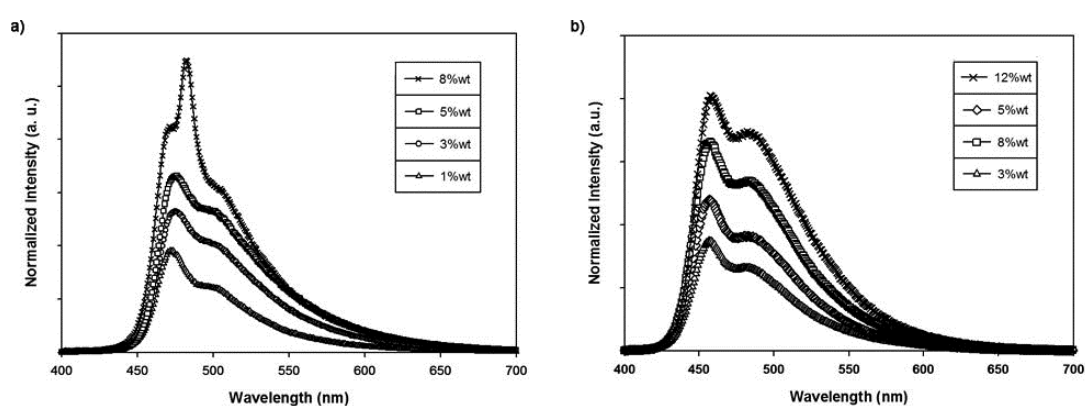


Figure 2 Normalized EL spectra operated at current density 0.1 mA/cm^2 of dopants: a) **15** and b) **18**

In Figure 2, the EL spectra of **15** show the emission peak at 475 and 482 nm for dopant concentrations $\leq 5\%$ and 8% , respectively. This 14 nm red shift between the diluted solution and doped OLED device at low concentration ($\leq 5\%$) can be due to aggregation effects in the solid. However, at high concentration (8%), the higher 21 nm red shift, as well as the unusual luminescent pattern, indicated excimer formation. Similarly, the EL spectra for **18** show the emission peak at 457 nm and a 14 nm red shift for every concentration (3-12%) of doped material and no excimer was observed. However, these results also confirm the solid state properties of pure dopants (Table 2) in which, the extension of π conjugated backbone on oligo-*p*PEs POSS lowers the π interaction between molecules as shown by a suppression of excimer.

Table 3 OLED device properties of dopants: a) **15** and b) **18**

a)

% wt of 15	EL _{max} (nm)	TV ^a	BV ^b	Current density (mA/cm ²) ^c	Luminous Efficiency (cd/A) ^d	EQE (%) ^e
1%	473	6.3	7.9	2.31	3.87	1.44
3%	475	6.4	8.0	2.49	3.96	1.47
5%	475	6.5	8.0	2.34	4.54	1.50
8%	482	5.9	7.8	3.47	2.86	1.34

b)

% wt of 18	EL _{max} (nm)	TV ^a	BV ^b	Current density (mA/cm ²) ^c	Luminous Efficiency (cd/A) ^d	EQE (%) ^e
3%	456	7.9	11.1	8.34	1.15	1.45
5%	457	7.8	9.7	4.03	2.51	1.66
8%	457	9.4	10.8	4.30	2.26	1.39
12%	457	6.7	9.3	2.59	3.76	1.73

^aTurn on voltage, ^ba bias voltage, ^cat 2 cd/m², ^dat the light forward output of 100 cd/m², and ^ethe external quantum efficiency

OLED devices properties for **15** and **18** are also summarized in Table 3. Devices having **15** as the dopant and the device A had a turn-on voltage about 5.9-6.5 V with a low brightness (~ 2 cd/m²). The maximum external quantum and luminous efficiencies of 1.50% and 4.54 cd/A, respectively, can be reached using 5% of dopant. Thus, a forward light output of 100 cd/m² was achieved at 8.0 V as well as a current density at 2.34 mA/cm². A different performance can be seen for the device B doped with **18**, where the turn-on voltage is around 6.7-9.4 V. The highest doped concentration of 12% shows the best device with the maximum quantum and luminous efficiencies at 1.73 and 3.76, respectively. Thus, a bias voltage of 9.3 V with a corresponding current density of 2.59 mA/cm² is needed to reach a forward light output of 100 cd/m².

3. Conclusions

We successfully demonstrated the synthesis and characterization of new classes of mono- and oligo(*p*-phenylene ethynylene)s end-capped with various polycyclic aromatics for tunable photoluminescence in the blue emission range and also grafting POSS as a pendant group. We have shown that these materials

derived from cubic silsesquioxanes are very robust with high $T_g > 80^\circ\text{C}$ and exhibit excellent thermal stabilities to air ($T_{5\% \text{ loss}} > 333^\circ\text{C}$). Thus, their optical properties all showed high photoluminescence with blue emission and quantum yield $> 80\%$ in the solution. In the solid state, we also found that the high order structure of extended conjugation system on *p*PE backbone tends to suppress the quenching process with a maintainable quantum yield. In OLED applications, we make a preliminary report of some of the materials as an active dopant in PVK and PBD matrix of multilayer OLEDs.

4. Experimental

4.1 Instruments

^1H (300 MHz), ^1H (500 MHz), ^{13}C (125 MHz), and ^{29}Si (99 MHz) NMR spectra were obtained in CDCl_3 on a Varian spectrometer model Unity INOVA. Chemical shifts are reported in ppm relative to CHCl_3 (δ 7.26, ^1H) and CDCl_3 (δ 77.0, ^{13}C). Matrix Assisted Laser Desorption Ionization Time of Flight Mass Spectrometry (MALDI-TOF MS) was performed using a Voyager-DE RP (Applied Biosystems) in linear mode. The matrix 2,5-dihydroxybenzoic acid (DHBA) was dissolved in THF (10 mg/mL), and mixed with the sample solution (0.5~1 mg/mL in THF) in 1:1 v/v ratio. The samples were spotted onto the target and dried in air. Elemental analyses were performed by CHNOS Elemental Analyzer, Vario EL III. Column chromatography (CC): SiO_2 60 (230~400 mesh, 40~63 μm) from E. Merck. TLC glass plates coated with SiO_2 60 F_{254} from E. Merck, visualization by UV light.

UV-Vis absorption spectra of materials were collected by JASCO, V-670 spectrometer. The PL and EL spectra and fluorescence quantum yield were measured by C9920-02 Hamamatsu spectrometer. The current density, voltage, and external quantum efficiency of OLED devices were determined by Keithley 4200 semiconductor parameter analyzer system and an integrating sphere equipped with a Si photodiode (S2281, Hamamatsu photonics). The luminous efficiency was analyzed by a luminance meter (BM-9, Topcon).

4.2 Materials

1-Ethynylpyrene, 9-ethynylphenanthrene, and 2-ethynyl-6-methoxynaphthalene, were commercially available through Aldrich and ((4-iodophenyl)ethynyl)trimethylsilane from Alfa Aesar company. Materials for OLED devices, the host polymer as poly(9-vinylcarbazole) (PVK) has a high molecular weight-average of 1,100,000 g/mole and electron-transporting molecule 2-(4-biphenyl)-5-phenyl-1,3,4-oxadiazole (PBD) were purchased from Aldrich. The high conductivity coating surface of poly(3,4-ethylenedioxythiophene)-poly(styrenesulfonate) formulation (PEDOT:PSS) were purchased from Baytron P, Al 4083. All materials were used as received without further purification.

4.3 Synthesis

4.3.1 Synthesis of 1,4-di(triazole-POSS) benzene (2). Under a nitrogen atmosphere, 1,4-bis(prop-2-ynyloxy)benzene (0.162 g, 0.87 mmol) and **3** (1.72 g, 1.91 mmol) were dissolved in 12 mL of THF. The flask was flushed with nitrogen, frozen, and evacuated for three times, after which $\text{CuSO}_4 \cdot 5\text{H}_2\text{O}$ (22 mg, 0.088 mmol) and sodium ascorbate (51.7 mg, 0.261 mmol) in 0.30 mL of degassed water were added. The reaction mixture was allowed to stir at 40°C for 2 days. The solution was filtered through cotton and evaporation of solvent giving a crude solid. The product was separated by column chromatography with elution in hexane:ethyl acetate (3:1) ($R_f = 0.25$) to obtain a white solid (1.62 g, 0.818 mmol, 94% yield). ^1H NMR (300 MHz, CDCl_3): $\delta = 7.57$ (s, 2H), 6.94 (s, 4H), 5.16 (s, 4H), 4.37 (t, $J = 7.5$ Hz, 4H), 2.01 (quin, $J = 7.8$ Hz, 4H), 1.89 (m, 14H), 0.96 (d, $J = 6.6$ Hz, 84H), 0.66 (overlapped, 4H), 0.63 (m, 28H); ^{13}C NMR (125 MHz, CDCl_3): δ 152.8, 144.3, 122.3, 115.7, 62.72, 52.57, 25.68, 25.66, 24.14, 23.87, 23.82, 22.43, 22.39, 9.24; ^{29}Si NMR (99 MHz, CDCl_3 , TMS): δ -67.55, -67.84, -68.59 (relative intensity ratio 3:4:1); MALDI-TOF MS [$\text{C}_{74}\text{H}_{148}\text{N}_6\text{O}_{26}\text{Si}_{16} + \text{Na}$] $^+$: Calcd. 2010.67, found 2010.11; Elemental analyses ($\text{C}_{74}\text{H}_{148}\text{N}_6\text{O}_{26}\text{Si}_{16}$): Calcd. C 44.72, H 7.51, N 4.23; Found C 44.65, H 7.63, N 4.21.

4.3.2 Synthesis of 2,5-diiodo-1,4-di(triazole-POSS) benzene (3). Under a nitrogen atmosphere, 1,4-diiodo-2,5-bis(prop-2-ynyloxy)benzene (0.6425 g, 1.70 mmol), and **3** (3.30 g, 3.664 mmol) were dissolved in 30 mL of THF. The reaction

flask was flushed with nitrogen, frozen, and evacuated three times, after which $\text{CuSO}_4 \cdot 5\text{H}_2\text{O}$ (160 mg, 0.64 mmol) and sodium ascorbate (380 mg, 1.92 mmol) in 0.50 mL of degassed water and Cu powder (0.10 g) were added. The solution mixture was refluxed for 5 days. The solution was filtered through cotton and the solvent evaporated to give a crude solid. The crude product was dissolved in a small amount of dichloromethane and separated by column chromatography with elution in hexane:ethyl acetate (4:1) ($R_f = 0.60$) to obtain white solid product (3.04 g, 1.36 mmol, 80% yield). ^1H NMR (300 MHz, CDCl_3): δ 7.67 (s, 2H), 7.38 (s, 2H), 5.20 (s, 4H), 4.39 (t, $J = 7.2$ Hz, 4H), 2.08 (quin, $J = 7.5$ Hz, 4H), 1.91 (m, 14H), 0.96 (d, $J = 6.6$ Hz, 84H), 0.67 (overlapped, 4H), 0.62 (m, 28H); ^{13}C NMR (125 MHz, CDCl_3): δ 152.7, 143.5, 123.7, 122.6, 86.58, 64.72, 52.67, 25.69, 24.25, 23.87, 23.82, 22.44, 22.41, 9.25; ^{29}Si NMR (99 MHz, CDCl_3 , TMS): δ -67.52, -67.84, -68.59 (relative intensity ratio 3:4:1); MALDI-TOF MS [$\text{C}_{74}\text{H}_{146}\text{I}_2\text{N}_6\text{O}_{26}\text{Si}_{16} + \text{Na}$] $^+$: Calcd. 2261.46, found 2261.69; Elemental analyses ($\text{C}_{74}\text{H}_{146}\text{I}_2\text{N}_6\text{O}_{26}\text{Si}_{16}$): Calcd. C 39.69, H 6.57, N 3.75; Found C 39.64, H 6.72, N 3.75.

4.3.3 General procedure for the synthesis of polycyclic aromatic derivatives (7, 8, and 9)

(4-(Iodophenyl)ethynyl)trimethylsilane (0.30 g, 0.999 mmol) and ethynyl polycyclic aromatic derivatives (**4**, **5**, or **6**) (1.20 mmol) were dissolved in tetrahydrofuran (13 mL) and piperidine (1 mL) in an oven-dried Schlenk flask. The flask was flushed with nitrogen after which $(\text{Ph}_3\text{P})_2\text{PdCl}_2$ (0.035 g, 0.05 mmol) and CuI (0.0095 g, 0.05 mol) were added. The mixture was allowed to stir at room temperature for overnight. The solvent was removed and the mixture was dissolved in dichloromethane and further washed with 0.5 M HCl and water. The organic layer was dried over Na_2SO_4 and evaporation of solvent gave a crude. The resulting products were purified by column chromatography and recrystallization.

4.3.3.1 7; Purification by flash chromatography on silica gel (Hexane/ CH_2Cl_2 1:1) $R_f = 0.74$ and further recrystallization in acetone; 255 mg (72% yield) as a colorless crystal. ^1H -NMR (500 MHz, CDCl_3): δ 7.97 (s, 1H), 7.69-7.60 (t, $J = 7.5$ Hz, 2H), 7.54 (m, 1H), 7.49 (m, 4H), 7.18 (m, 1H), 7.12 (s,

1H), 3.93 (s, 3H), 0.262 (s, 9H); ^{13}C NMR (125 MHz, CDCl_3) δ 158.4, 134.2, 131.89, 131.48, 131.36, 131.31, 131.28, 129.46, 129.28, 128.93, 128.85, 128.45, 126.95, 126.77, 125.52, 122.69, 119.47, 117.82, 105.78, 104.68, 96.95, 91.95, 88.73, 55.37, 55.33, -0.074, -0.101; MALDI-TOF MS [$\text{C}_{24}\text{H}_{22}\text{OSi} + \text{H}$] $^+$: Calcd. 355.15, found 355.1; Elemental analyses ($\text{C}_{24}\text{H}_{22}\text{OSi}$): Calcd. C 81.31, H 6.25; Found C 81.25, H 6.46.

4.3.3.2 **8**; Purification by recrystallization in acetone; 285 mg (76% yield) as light yellow solid. ^1H -NMR (500 MHz, CDCl_3): δ 8.72 (m, 1H), 8.68 (d, $J = 8.0$ Hz, 1H), 8.53 (m, 1H), 8.09 (s, 1H), 7.89 (d, $J = 7.5$, 1H), 7.73-7.67 (m, 3H), 7.63 (m, 1H), 7.62 (m, 2H), 7.52 (m, 2H), 0.28 (s, 9H); ^{13}C NMR (125 MHz, CDCl_3) δ 132.1, 131.9, 131.5, 131.2, 130.9, 130.4, 130.1, 128.6, 127.59, 127.14, 127.12, 127.00, 126.9, 123.4, 123.1, 122.8, 122.6, 119.4, 104.6, 96.4, 93.5, 89.7, -0.074; MALDI-TOF MS [$\text{C}_{27}\text{H}_{22}\text{Si} + \text{H}$] $^+$: Calcd. 375.16, found 375.2; Elemental analyses ($\text{C}_{27}\text{H}_{22}\text{Si}$): Calcd. C 86.58, H 5.92; Found C 86.44, H 5.68.

4.3.3.3 **9**; Purification by flash chromatography on silica gel (Hexane/ CH_2Cl_2 10:1) $R_f = 0.35$ and further recrystallization in acetone; 276 mg (69% yield) as yellow solid. ^1H -NMR (500 MHz, CDCl_3): δ 8.65 (d, $J = 9.5$ Hz, 1H), 8.24-8.02 (m, 8H), 7.66 (m, 2H), 7.54 (m, 2H), 0.29 (s, 9H); ^{13}C NMR (125 MHz, CDCl_3) δ 132.0, 131.91, 131.44, 131.39, 131.22, 131.03, 129.6, 128.4, 128.3, 127.2, 126.3, 125.70, 125.65, 125.42, 124.53, 124.46, 124.28, 123.6, 122.9, 117.4, 104.7, 96.4, 94.8, 90.6, -0.062; MALDI-TOF MS [$\text{C}_{29}\text{H}_{22}\text{Si} + \text{H}$] $^+$: Calcd. 399.16, found 399.2; Elemental analyses ($\text{C}_{29}\text{H}_{22}\text{Si}$): Calcd. C 87.39, H 5.56; Found C 87.22, H 5.47.

4.3.4 General procedure for the deprotection of polycyclic aromatic derivatives (10, 11, and 12)

Compounds (**7**, **8** or **9**) (0.20 g) was dissolved in THF (15 ml), followed by methanol (5 mL). The flask was flushed with nitrogen after which K_2CO_3 (0.020 g) as a catalytic methanolysis was added and kept stirring for an hour. Evaporation of solvent gave the crude of deprotected products, further washed with dionized

water, filter, and dried. The products (**10**, **11**, or **12**) were used through next step without further purification.

4.3.5 General procedure for the synthesis of mono- and oligo(*p*-phenylene ethynylene)s end-capping with polycyclic aromatics (13-18)

2-arm POSS monomer (**3**) (0.20 g, 0.0894 mmol) and polycyclic derivatives (**4**, **5**, **6**, **10**, **11**, or **12**) (0.210 mmol) were dissolved in THF (6 mL) and piperidine (0.6 mL) in an oven-dried Schlenk flask. The flask was flushed with nitrogen after which $(\text{Ph}_3\text{P})_2\text{PdCl}_2$ (3.2 mg, 0.00459 mmol) and CuI (1.8 mg, 0.00918 mmol) were added. The mixture was allowed to stir at room temperature overnight, after which the solvent was removed. The crude mixture was dissolved in dichloromethane and washed with 0.5 M HCl and water. The organic layer was dried over Na_2SO_4 and the solvent was removed. The resulting product was purified by column chromatography.

4.3.5.1 13; Purification by flash chromatography on silica gel with gradient eluent (CH_2Cl_2 and CH_2Cl_2 /ethylacetate 100:1) $R_f = 0.45$ provided a light yellow solid (197 mg, 0.0840 mmol, 94% yield). $^1\text{H-NMR}$ (300 MHz, CDCl_3): δ 7.98 (s, 2H), 7.73-7.69 (m, 4H), 7.66 (s, 2H), 7.55 (m, 2H), 7.23 (s, 2H), 7.19-7.16 (m, 2H), 7.13 (m, 2H), 5.36 (s, 4H), 4.33 (t, $J = 7.2$ Hz, 4H), 3.94 (s, 6H), 2.02 (pent, $J = 7.8$ Hz, 4H), 1.88-1.75 (m, 14H), 0.96-0.91 (m, 84H), 0.64 (overlapped, 4H), 0.59 (d, $J = 7.2$ Hz, 28H); $^{13}\text{C-NMR}$ (125 MHz, CDCl_3) δ 158.4, 153.4, 144.3, 134.2, 131.4, 129.4, 128.9, 128.5, 126.8, 122.4, 119.5, 118.3, 118.0, 114.8, 105.8, 96.1, 85.2, 64.4, 55.3, 52.6, 25.7, 25.6, 24.2, 23.84, 23.80, 22.42, 22.36, 9.28; MALDI-TOF MS $[\text{C}_{100}\text{H}_{164}\text{N}_6\text{O}_{28}\text{Si}_{16} + \text{Na}]^+$: Calcd. 2368.78, found 2369.14; Elemental analyses ($\text{C}_{100}\text{H}_{164}\text{N}_6\text{O}_{28}\text{Si}_{16}$): Calcd. C 51.16, H 7.04, N 3.58; Found C 51.45, H 7.34, N 3.77.

4.3.5.2 14; Purification by flash chromatography on silica gel with gradient solvent (CH_2Cl_2 and CH_2Cl_2 /ethylacetate 100:1) $R_f = 0.65$ provided a yellow solid (0.186 g, 0.0780 mmol, 87% yield). $^1\text{H NMR}$ (300 MHz, CDCl_3): δ 8.72 (t, $J = 9.0$ Hz, 4H), 8.58 (d, $J = 8.1$ Hz, 2H), 8.12 (s, 2H) 7.91 (m, 2H), 7.70-7.62 (m, 6H), 7.67 (overlapped, 2H), 7.54 (t, $J = 7.8$ Hz, 2H), 7.39 (s, 2H), 5.45 (s, 4H),

4.26 (t, $J = 7.2$ Hz, 4H), 1.95 (m, 4H), 1.88 (m, 14H), 0.96 (m, 84H), 0.60 (m, 28H), 0.54 (overlapped, 4H); ^{13}C -NMR (125 MHz, CDCl_3) δ 153.7, 143.9, 131.8, 131.2, 131.0, 130.4, 130.1, 128.7, 127.6, 127.2, 127.1, 127.02, 127.03, 122.8, 122.7, 122.6, 119.6, 117.2, 114.6, 94.2, 90.2, 64.0, 52.6, 25.7, 25.6, 24.1, 23.83, 23.80, 22.4, 22.3, 9.27; MALDI-TOF MS [$\text{C}_{106}\text{H}_{164}\text{N}_6\text{O}_{26}\text{Si}_{16} + \text{Na}$] $^+$: Calcd. 2408.79, found 2409.00; Elemental analyses ($\text{C}_{106}\text{H}_{164}\text{N}_6\text{O}_{26}\text{Si}_{16}$): Calcd. C 53.32, H 6.92, N 3.52; Found C 53.11, H 7.05, N 3.72.

4.3.5.3 **15**; Purification by flash chromatography on silica gel with gradient eluent (CH_2Cl_2 and $\text{CH}_2\text{Cl}_2/\text{ethylacetate}$ 100:1) $R_f = 0.70$ provided a yellow solid (182 mg, 0.0748 mmol, 84% yield). ^1H -NMR (300 MHz, CDCl_3): δ 8.70 (d, $J = 9.0$ Hz, 2H), 8.25-8.03 (m, 16H), 7.73 (s, 2H), 7.44 (s, 2H), 5.50 (s, 4H), 4.24 (t, $J = 7.5$ Hz, 4H), 1.97 (m, 4H), 1.85 (m, 14H), 0.95 (m, 84H), 0.59 (m, 28H), 0.50 (overlapped, 2H); ^{13}C -NMR (125 MHz, CDCl_3) δ 153.6, 144.0, 132.1, 131.4, 131.3, 131.1, 129.4, 128.3, 127.3, 126.3, 125.8, 125.6, 124.6, 124.5, 124.3, 122.8, 117.7, 117.2, 114.8, 95.2, 91.5, 64.1, 52.6, 25.7, 25.6, 24.0, 23.8, 22.4, 22.3, 9.21; MALDI-TOF MS [$\text{C}_{110}\text{H}_{164}\text{N}_6\text{O}_{26}\text{Si}_{16} + \text{Na}$] $^+$: Calcd. 2455.79 found 2456.53; Elemental analyses ($\text{C}_{110}\text{H}_{164}\text{N}_6\text{O}_{26}\text{Si}_{16}$): Calcd. C 54.24, H 6.79, N 3.45; Found C 54.38, H 6.55, N 3.49.

4.3.5.4 **16**; Purification by flash chromatography on silica gel with gradient eluent (CH_2Cl_2 and $\text{CH}_2\text{Cl}_2/\text{ethylacetate}$ 100:1) $R_f = 0.55$ provided light yellow crystals (212 mg, 0.0832 mmol, 93% yield). ^1H -NMR (300 MHz, CDCl_3): δ 7.99 (s, 2H), 7.74-7.70 (m, 4H), 7.63 (s, 2H), 7.56-7.50 (m, 2H), 7.53-7.52 (overlapped, 8H), 7.21 (s, 2H), 7.19-7.16 (m, 2H), 7.13 (m, 2H), 5.33 (s, 4H), 4.37 (t, $J = 7.2$ Hz, 4H), 3.94 (s, 6H), 2.05 (pent, $J = 8.1$ Hz, 4H), 1.87 (m, 14H), 0.96 (m, 84H), 0.67 (overlapped, 4H), 0.61 (m, 28H); ^{13}C -NMR (125 MHz, CDCl_3) δ 158.4, 153.4, 144.1, 134.2, 131.6, 131.49, 131.41, 131.39, 128.9, 128.5, 126.9, 123.6, 122.73, 122.42, 119.5, 118.2, 117.8, 114.7, 105.8, 95.3, 92.2, 88.8, 87.3, 64.2, 55.4, 52.6, 25.7, 25.6, 24.2, 23.9, 23.8, 22.42, 22.37, 9.28; MALDI-TOF MS [$\text{C}_{116}\text{H}_{172}\text{N}_6\text{O}_{28}\text{Si}_{16} + \text{Na}$] $^+$: Calcd. 2569.85, found 2570.56; Elemental analyses ($\text{C}_{116}\text{H}_{172}\text{N}_6\text{O}_{28}\text{Si}_{16}$): Calcd. C 54.68, H 6.80, N 3.30; Found C 54.55, H 6.78, N 3.32.

4.3.5.5 **17**; purification by flash chromatography on silica gel with gradient eluent (CH₂Cl₂ and CH₂Cl₂/ethylacetate 100:1) $R_f = 0.70$ provided a yellow solid (0.220 mg, 0.0851 mmol, 95% yield). ¹H-NMR (500 MHz, CDCl₃): δ 8.74 (m, 2H), 8.69 (d, $J = 8.0$ Hz, 2H), 8.55 (m, 2H), 8.11 (s, 2H), 7.90 (d, $J = 7.0$ Hz, 2H), 7.74-7.61 (m, 8H), 7.674-7.659 (d (overlapped), $J = 7.5$ Hz, 4H), 7.648 (s (overlapped), 2H), 7.58-7.57 (d, $J = 8.5$ Hz, 4H), 7.24 (s, 2H), 5.36 (s, 4H), 4.38 (t, $J = 7.5$ Hz, 4H), 2.04 (pent, $J = 7.5$ Hz, 4H) 1.87 (oct; $J = 6.0$ Hz, 14H), 0.95 (m, 84H), 0.66 (overlapped, 4H), 0.61 (t, $J = 6.0$ Hz, 28H); ¹³C-NMR (125 MHz, CDCl₃) δ 153.4, 144.1, 132.2, 132.0, 131.74, 131.69, 131.59, 131.54, 131.2, 130.9, 130.4, 130.1, 128.7, 128.5, 127.7, 127.3, 127.1, 127.0, 123.4, 123.1, 122.8, 122.5, 122.3, 119.4, 118.3, 114.7, 95.3, 93.6, 89.8, 87.5, 64.2, 52.6, 26.1, 25.7, 25.6, 25.1, 24.2, 23.91, 23.85, 23.82, 23.76, 22.42, 22.38, 9.28; MALDI-TOF MS [C₁₂₂H₁₇₂N₆O₂₆Si₁₆ + Na]⁺: Calcd. 2609.86, found 2610.63; Elemental analyses (C₁₂₂H₁₇₂N₆O₂₆Si₁₆): Calcd. C 56.62, H 6.70, N 3.25; Found C 56.91, H 6.58, N 3.11.

4.3.5.6 **18**; Purification by flash chromatography on silica gel with gradient eluent (CH₂Cl₂ and CH₂Cl₂/ethylacetate 100:1) $R_f = 0.75$ provided a yellow solid product (235 mg, 0.0892 mmol, 99% yield). ¹H-NMR (300 MHz, CDCl₃): δ 8.68 (d, $J = 9.3$ Hz, 2H), 8.24-8.05 (m, 16H), 7.72 (d, $J = 8.7$ Hz, 4H), 7.669 (s, 2H), 7.61 (d, $J = 8.4$ Hz, 4H), 7.25 (s, 2H), 5.37 (s, 4H), 4.37 (t, $J = 7.2$ Hz, 4H), 2.07 (pent, $J = 7.5$ Hz, 4H), 1.84 (m, 14H), 0.95 (d, $J = 6.0$ Hz, 84H), 0.68 (overlapped, 4H), 0.62 (m, 28H); ¹³C-NMR (125 MHz, CDCl₃) δ 153.3, 144.1, 131.9, 131.7, 131.6, 131.5, 131.2, 131.0, 129.6, 128.4, 128.3, 127.2, 126.3, 125.7, 125.4, 124.6, 124.5, 124.3, 123.6, 123.0, 122.5, 118.3, 117.4, 114.7, 95.4, 94.8, 90.8, 87.5, 64.2, 52.7, 25.6, 24.2, 23.9, 23.8, 22.4, 22.3, 9.30; MALDI-TOF MS [C₁₂₆H₁₇₂N₆O₂₆Si₁₆ + Na]⁺: Calcd. 2657.86, found 2657.59; Elemental analyses (C₁₂₆H₁₇₂N₆O₂₆Si₁₆): Calcd. C 57.41, H 6.58, N 3.19; Found C 57.37, H 6.44, N 3.39.

4.4 Fabrication of EL devices A and B

4.4.1 Device A

The multilayer OLED with ITO/PEDOT:PSS/PVK:PBD:Dopant/MPT/LiF/Al structure was fabricated. Before applying materials by a spin coating method on indium tin oxide (ITO) covered glass substrates, the substrates were cleaned using consecutive ultrasonic baths of

acetone (10 min), Semico detergent (10 min), water (10 min), and isopropanol (10 min). Then, the substrates were treated by UV ozone for 30 min. PEDOT:PSS solution was spin-coated onto the ITO surface with a typical spinning speed and time at 1600 rpm and 30 s, respectively. The film coat was then dried over the hot plate 120°C for 10 min, giving 60 nm of thickness. PVK and PBD in a weight ratio of 3:2, followed by additional concentration of dopant emitters (**15**) at 1%, 3%, 5%, and 8% of total weight, were dissolved in chlorobenzene solution with total solid concentration of 15 mg/ml. The mixture solution was then spin-coated onto the PEDOT:PSS surface with 1600 rpm for 30 s giving 60 nm of thickness, followed by heating at 70°C for 10 minutes in a nitrogen-filled glove box and then immediately transferred into a vacuum for deposition. 2,4-bis-biphenyl-4-yl-6-(4'-pyridin-2-yl-biphenyl-4-yl)-[1,3,5]triazine (MPT) (30 nm), LiF (0.5 nm), and Al (100 nm) cathode were deposited layer by layer on top of a spin-coating device by the thermal evaporation, respectively.

4.4.2 Device B

The multilayer OLED with ITO/PEDOT:PSS/PVK/PVK:PBD:Dopant/MPT/LiF/Al structure was fabricated. The substrate ITO was cleaned following as a treatment of device (A) . PEDOT:PSS solution was spin-coated onto the ITO surface with a typical thickness 60 nm and then dried over the hot plate 120°C for 10 min. Pure PVK in chlorobenzene solution (10 mg/ml) was spin-coated on top of PEDOT:PSS to obtain a 50 nm of thickness and quickly moved to nitrogen-filled glove box for drying at 70°C for 10 minutes. PVK and PBD in a weight ratio of 3:2, followed by additional concentration of dopant emitters (**18**) at 3%, 5%, 8%, and 12% of total weight, were dissolved in chlorobenzene solution with total solid concentration of 15 mg/ml. The mixture solution was then spin-coated onto the PVK surface with 1600 rpm for 30 s giving about 60 nm of thickness, followed by heating at 70°C for 10 minutes in a nitrogen-filled glove box and then immediately transferred into a vacuum for deposition. MPT (30 nm), LiF (0.5 nm), and Al (100 nm) cathode were deposited layer by layer on top of a spin-coating device by the thermal evaporation, respectively.

Acknowledgement

V. Ervithayasuporn and X. Wang thank to Ministry of Education, Culture, Sports, Science, and Technology (MEXT), Japanese Government for supporting a scholarship at JAIST.

References and notes

Supporting Information available for ¹H-NMR spectra and TGA profiles of materials.

1. Grimsdale, A.C.; Müllen, K. *Adv. Polym. Sci.* **2006**, *199*, 1.
2. Grimsdale, A.C.; Chan, K.L.; Martin, R.E.; Jokisz, P.G.; Holmes, A.B. *Chem. Rev.* **2009**, *109*, 897.
3. McQuade, D.T.; Pullen, A.E.; Swager, T.M. *Chem. Rev.* **2000**, *100*, 2537.
4. Thomas, S.W.; Joly, G.D.; Swager, T.M. *Chem. Rev.* **2007**, *107*, 1339.
5. Mwaura, J.K.; Zhao, X.; Jiang, H.; Schanze, K.S.; Reynolds, J.R. *Chem. Mater.* **2006**, *18*, 6109.
6. Matsunaga, Y.; Takechi, K.; Akasaka, T.; Ramesh, A.R.; James, P.V.; Thomas, K.G.; Kamat, P.V. *J. Phys. Chem. B* **2008**, *112*, 14539.
7. Blaskskær, P.; Gothelf, K.V. *Org. Biomol. Chem.* **2006**, *4*, 3442.
8. Yang, L.; Gordon, V.D.; Mishra, A.; Som, A.; Purdy, K.R.; Davis, M.A.; Tew, G.N.; Wong, G.C.L. *J. Am. Chem. Soc.* **2007**, *129*, 12141.
9. Maillou, T.; Moigne, J.L.; Geffroy, B.; Lorin, A.; Rosilio, A.; Dumarcher, V.; Rocha, L.; Denis, C.; Fiorini, C.; Nunzi, J.-M. *Synth. Metals* **2001**, *124*, 87.
10. Breen, C.A.; Rifai, S.; Bulovic, V.; Swager, T.M. *Nano Lett.* **2005**, *4*, 1597.
11. Gin, M.S.; Moore, J.S. *Org. Lett.* **2000**, *2*, 135.
12. Hill, D.J.; Moore, J.S. *Proc. Natl. Acad. Sci.* **2002**, *99*, 5053.
13. Xue, C.; Luo, F.-T. *Tetrahedron* **2004**, *60*, 6285.
14. Cho, J.; Zhao, Y.; Tykwinski, R.R. *ARKIVOC* **2005**, *iv*, 142.
15. Hu, W.; Zhu, N.; Tang, W.; Zhao, D. *Org. Lett.* **2008**, *10*, 2669.
16. Atienza, C.; Martin, N.; Wielopolski, M.; Haworth, N.; Clark, T.; Guldi, D.M. *Chem. Comm.* **2006**, 3202.
17. McCusker, C.; Carroll, J. B.; Rotello, V.M. *Chem. Commun.* **2005**, 996.
18. Iacono, S.T.; Vij, A.; Grabow, W.; Smith, D.W.; Mabry, J.M. *Chem. Commun.* **2007**, 4992.

19. Kolel-Veetil, M.K.; Dominguez, D.D.; Klug, C.A.; Keller, T.M. *Macromolecules* **2009**, *42*, 3992.
20. Hoque, M.A.; Kakihana, Y.; Shinke, S.; Kawakami, Y. *Macromolecules* **2009**, *42*, 3309.
21. Xiao, S.; Nguyen, M.; Gong, X.; Cao, Y.; Wu, H.; Moses, D.; Heeger, A.J. *Adv. Funct. Mater.* **2003**, *13*, 25.
22. Imae, I.; Kawakami, Y. *J. Mater. Chem.* **2005**, *15*, 4581.
23. Cho, H.-J.; Hwang, D.-H.; Lee, J.-I.; Jung, Y.-K.; Park, J.-H.; Lee, J.; Lee, S.-K.; Shim, H.-K. *Chem. Mater.* **2006**, *18*, 3780.
24. Froehlich, J.D.; Young, R.; Nakamura, T.; Ohmori, Y.; Li, S.; Mochizuki, A.; Lauters, M.; Jabbour, G.E. *Chem. Mater.* **2007**, *19*, 4991.
25. Sellinger, A.; Tamaki, R.; Laine, R.M.; Ueno, K.; Tanabe, H.; William, E.; Jabbour, G.E. *Chem. Commun.* **2005**, 3700.
26. Lo, M.Y.; Zhen, C.; Lauters, M.; Jabbour, G.E.; Sellinger, A. *J. Am. Chem. Soc.* **2007**, *129*, 5808.
27. Laine, R.M.; Roll, M.; Asuncion, M.; Sulaiman, S.; Popova, V.; Bartz, D.; Krug, D.J.; Mutin, P.H. *J. Sol-Gel Sci. Technol.* **2008**, *46*, 335.
28. He, C.B.; Xiao, Y.; Huang, J.C.; Lin, T.T.; Mya, K.Y.; Zhang, X.H. *J. Am. Chem. Soc.* **2004**, *126*, 7792.
29. Xiao, Y.; Liu, L.; He, C.-B.; Chin, W.S.; Lin, T.T.; Mya, K.Y.; Huang, J.C.; Lu, X.H. *J. Mater. Chem.* **2006**, *16*, 829.
30. Miyake, J.; Chujo, Y. *Macromol. Rapid Commun.* **2008**, *29*, 86.
31. Miyake, J.; Chujo, Y. *J. Polym. Sci., Part A: Polym. Chem.* **2008**, *46*, 6035.
32. Miyake, J.; Chujo, Y. *J. Polym. Sci., Part A: Polym. Chem.* **2008**, *46*, 8112.
33. Ervithayasuporn, V.; Wang, X.; Kawakami, Y. *Chem. Comm.* **2009**, 5130.
34. Xue, C.; Luo, F.-T. *Tetrahedron* **2004**, *60*, 6285.
35. Sudeep, P.K.; James, P.V.; Thomas, K.G.; Kamat, P.V. *J. Phys. Chem. A* **2006**, *110*, 5642.
36. Zhao, X.; Pinto, M.R.; Hardison, L.M.; Mwaura, J.; Muller, J.; Jiang, H.; Witker, D.; Kleiman, V.D.; Reynolds, J.R.; Schanze, K.S. *Macromolecules* **2006**, *39*, 6355.